A&A 370, 273–280 (2001)
DOI: 10.1051/0004-6361:20010228

Astronomy & Astrophysics

Polar surges and macrospicules

II. Dynamics of an eruptive event from off-limb observations⋆

A. A. Georgakilas[1], S. Koutchmy[2], and E. B. Christopoulou[3]

[1] Solar Astronomy, California Institute of Technology, Pasadena, CA 91125, USA
[2] Institut d'Astrophysique de Paris, CNRS, 98bis boulevard Arago, 75014 Paris, France
e-mail: koutchmy@iap.fr
[3] Electronics Laboratory, University of Patras, Patras 26110, Greece
e-mail: echris@physics.upatras.gr

Received 15 December 2000 / Accepted 23 January 2001

Abstract. We continue our study of polar surges and macrospicules at the period of solar minimum, analyzing high resolution multiwavelength limb observations that provide a clearer picture of the dynamical phenomena occurring well above the chromosphere of a polar cap. The time sequence of an erupting and impulsive polar event is examined from the low chromosphere to coronal heights, deriving both proper motions and Doppler velocities. Our observations suggest that there is a close association of polar surges with explosive events, supporting the hypothesis that magnetic reconnection triggered by emerging flux provides the accelerative mechanism for this polar region event.

Key words. Sun: chromosphere, transition region

1. Introduction

Eclipse observers have repeatedly reported the presence of chromospheric extensions above polar regions as seen in broad band images during the totality, which means at coronal levels. Similar phenomena were studied in Hα using large coronographs (e.g. Koutchmy & Loucif 1991). During the Skylab mission, giant spikelike structures were observed in He II 304 Å spectroheliograms (Bohlin et al. 1975; Moe et al. 1975). They were called *macrospicules* and related to small, surge-like, quiet region Hα limb eruptions, with dimensions significantly larger than those of the usual Hα spicules (Moore et al. 1977). Moore et al. found that some macrospicules coincided with flaring X-ray bright points regions.

EIT (Extreme ultraviolet Imaging Telescope) on board SOHO gave the opportunity for new studies of the association of He II macrospicules to the Hα ones (Wang 1998; Georgakilas et al. 1999). Georgakilas et al. (1999) (referred to from now on as Paper I) from simultaneous sequences of Hα and He II 304 Å images, proposed to distinguish *Polar surges* and giant spicules (macrospicules) among the He II structures observed beyond the solar limb. Figures 3 and 4 in Paper I show the appearance and evolution of a characteristic example of this class of macrospicules, that we are referred to, using the term "polar surges" (introduced in the literature by Godoli & Mazzuconi 1967, and adopted from Moore et al. 1977). Zirin & Cameron (1988) referred to these phenomena as a class of macrospicules, naming them eruptions.

Blake & Sturrock (1985), adopting the position that spicules, macrospicules and surges are manifestations of the same phenomenon occurring on different scales, searched for a mechanism to explain the phenomenon on all three scales. They proposed that the driving force is magnetic. They further suggested that two different magnetic field configurations are required, one of which is subject to reconnection and provides the driving force, while the other provides the guidance necessary to explain the collimation observed in material ejection.

A number of authors have related normal-size surges or macrospicules with magnetic reconnection. Kurokawa & Kawai (1993), from the examination of the morphological and evolution characteristics of surges (occurring nearby Emerging Flux Regions (EFR)), concluded that they are produced by the magnetic field reconnection between the EFR and the pre-existing surrounding region. Gaizauskas (1996) presented an example of a surge observed in Hα supporting the notion that magnetic reconnection provides the accelerative mechanism for this phenomenon. Chae et al. (1999) from simultaneous EUV and Hα observations found EUV jets with a typical size of 4–10 Mm and a transverse velocity of 50–100 km s^{-1}, that they related to Hα surges. From their *solar disk* study they

Send offprint requests to: A. A. Georgakilas,
e-mail: ageorg@caltech.edu

⋆ Based on observations performed on the NSO/SPO Richard B. Dunn Solar Telescope (DST).

Fig. 1. Yohkoh soft X-ray image (taken a few hours after the eruptive event) showing the region where the polar surge occurred (Courtesy of ISAS and Lockheed group at Stanford University). The region was near the boundaries of the North pole Coronal hole and at the place where an X-ray bright point is obvious

concluded that Hα surges and EUV jets represent different kinds of plasma ejection – cool and hot plasma ejection along different field lines – which is a result of the "cancellation of the colliding magnetic fluxes". However they do not specify the origin of magnetic fluxes, due to projection effects.

2. Observations and image processing

In the frame of the Joint Observing Program 57, observations were obtained with the Extreme Ultraviolet Imaging Telescope on board SOHO and the Richard B. Dunn Solar Telescope (DST) of the Sacramento Peak Observatory on December 1996 and August 1997. The observations obtained on December 1996 are described in Paper I and references in there; the run of August 1997 is a repetition of the one of December 1996. In this work we study the dynamics of polar surges using exceptionally high resolution observations of a polar surge observed at Hα center, Hα -0.75 Å, Hα $+0.75$ Å, Mgb1-0.4, He I D_3 (5876 Å) and a nearby continuum. The observations were taken on August 15 1997. They cover a field of view $133''$ by $133''$ near the solar limb (N 66.6, E92.1). The polar surge was observed near the edge of a coronal hole. In the same region a bright point was obvious in a soft X-ray image taken a few hours after the eruptive event (Fig. 1, 22:30 UT). Simultaneous Fe XII 195 Å images obtained with the EIT are of low cadence (12 min) and low resolution ($5.12''$). A brightening was observed near the region of the polar surge, but the identification of the two events is not certain since their alignment with the Hα images presents difficulties due to the lack of good correlation between the images.

Raw images were corrected for dark current and flat field and carefully aligned. We furthermore normalized the images by computing the average intensity over a large area and dividing the intensity of each pixel by this value. Finally we applied a method for the improvement of the visibility of fine structures, based on the combination of a method for the correction of limb darkening (cf. Paper I) with a method for the enhancement of their contrast using a version of Madmax, a directionally sensitive operator (Koutchmy et al. 1989). For an analytical description of the method, see Christopoulou et al. (2001).

3. Analysis of high resolution observations of a polar surge

From a review of previous reports and from the present work, the main morphological characteristics of polar surges are (Paper I, Moore et al. 1977; Koutchmy & Loucif 1991; Loucif et al. 1998):

1) In Hα they begin as small bright bubbles that subsequently erupt;

2) They consist of one or more usually overlapping mount-like features;

3) They show not only a vertical but also a transverse expansion;

4) After the main phase of the eruption and as they decay, a complex structure of loops and bright blobs (small roundish clouds of material) are observable;

5) They show emission in both Hα and He II 304 Å lines.

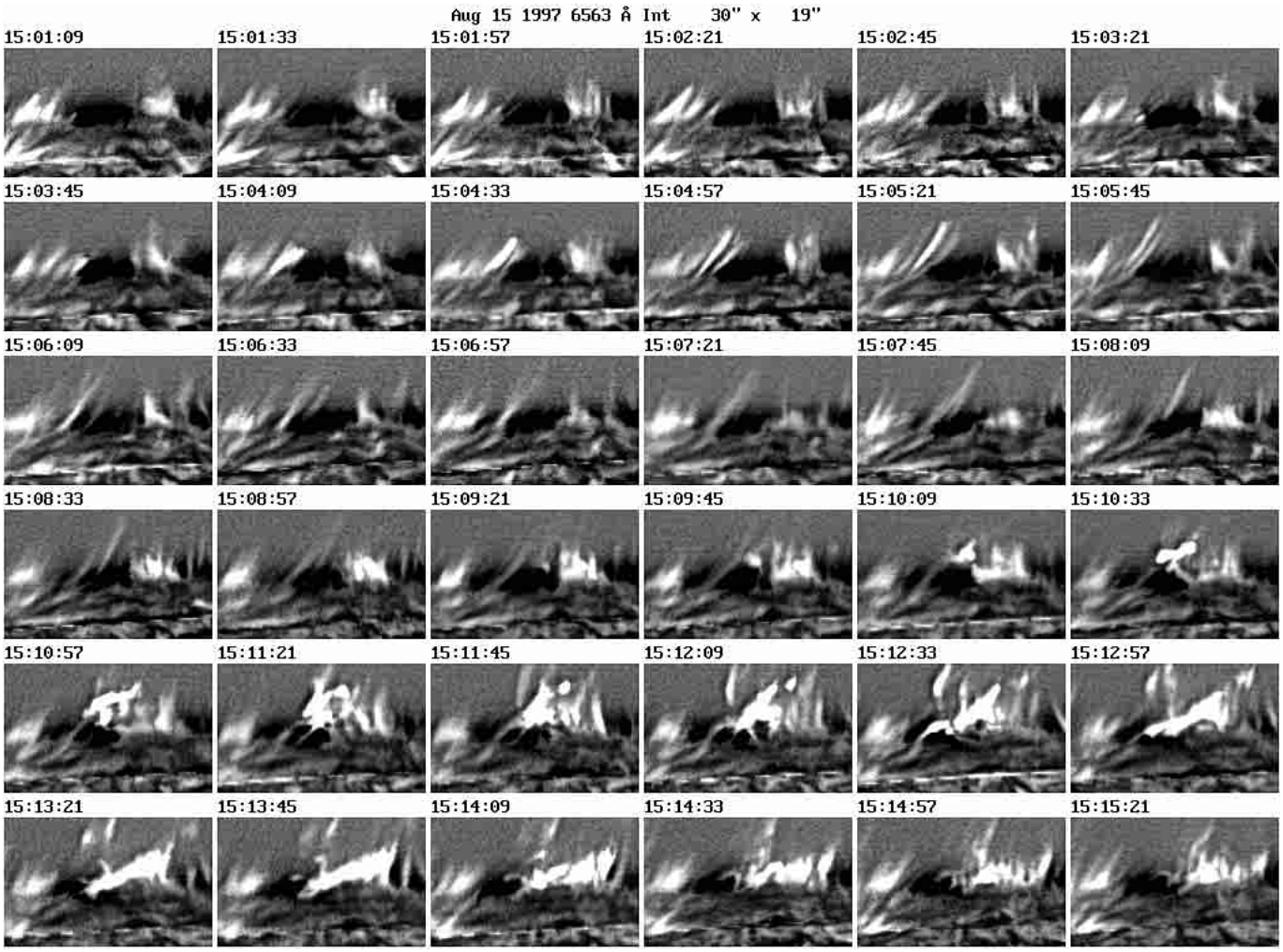

Fig. 2. Hα center filtergrams showing the appearance, development and decay of a polar surge observed on August 15, 1997. The sampling time is 24 s. Note that the chromospheric fringe is optically too thick, restricting the visualization of the structures down to the surface of the Sun

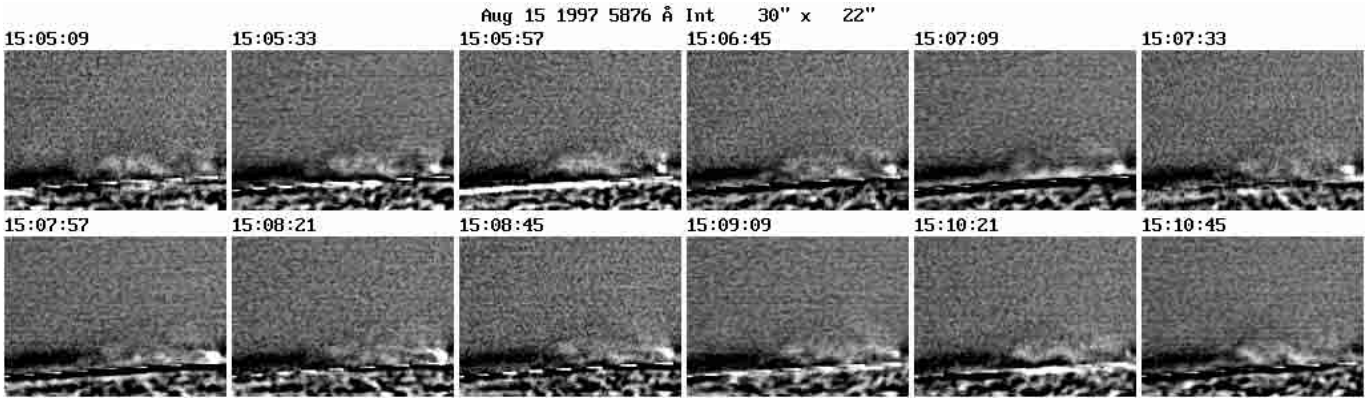

Fig. 3. Filtergrams in He I D_3 (5876 Å) line, during the main phase of the development of the polar surge. Compare with Fig. 4 and note the small brightening close to the surface of the Sun, to the right of the frame

In most cases they appear in He II 304 Å well before Hα and remain visible longer during the decay phase;
6) They tend to re-occur at the same place.

We now describe the detailed evolution and the dynamics of the polar surge.

3.1. Overview of the evolution of the polar surge

Figures 2–4 show the appearance, development and decay of the polar surge, observed in Hα center, He I D_3 and Hα + 0.75 Å respectively. The appearance of the polar surge in the red wing is completely different from that in the line

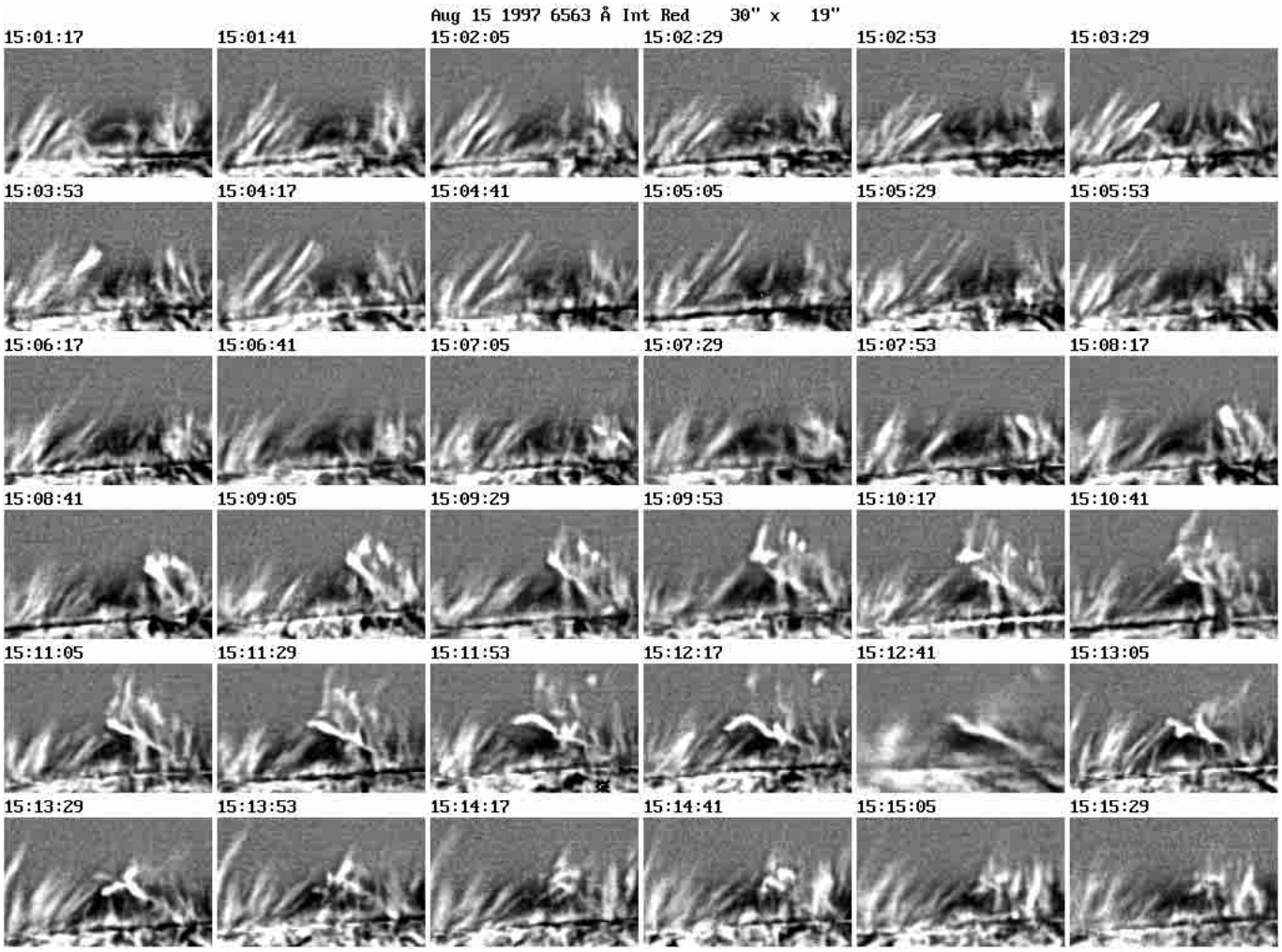

Fig. 4. Hα + 0.75 Å filtergrams showing the development of the same surge as in Fig. 2. The fine structure of the phenomenon can be observed (see text for a description)

center. When we observe at the line center, the lower part of the limb is obscured and what we really observe is the middle and upper part of the polar surge. Observations in far wings give us the opportunity to observe the lower part of the polar surge and thus the initial phases of the phenomenon.

It is clear that the event is not a single spike ejection; it is a complex process. The polar surge is evolving over a dark mount-like region with spicules around it forming an inverted "Y" configuration. *Before* the main phenomenon we observe the appearance and elongation of a so-called twin spicule on the left side of the configuration (Fig. 2). The twin spicule appears at about 15:03:45 UT; after a brightening (15:04:33) it starts elongating towards the right side of the configuration.

At Hα center, the main phase begins with an intense brightening that appears at about the middle of the mountlike region (Fig. 2: 15:09:45) at a height of about 6.5 Mm above the photospheric limb. However, an intense brightening observed at the He I D_3 line at about 15:05:33 (Fig. 3) suggests that a precursor phenomenon starts earlier. From the red wing, we can see that indeed the phenomenon begins with the emergence of a loop like feature that is already obvious at 15:06:17; it is more clearly discernible at 15:08:17 UT. The material is not uniformly distributed along the loop-like feature, but is ascending in the form of blobs or concentrations.

As soon as the loop-like feature reaches a certain point above the dark mountlike region and almost in contact with the remnants of the twin spicule (Fig. 2: 15:09:45, Fig. 4: 15:09:53), the brightening at Hα center appears. Subsequently the brightening expands and we observe the formation of several threads and of a blob of material (15:11:21–15:12:33). Further we observe the formation of a loop at the base of the configuration (Fig. 2: 15:12:09); it appears to be formed from part of the remnants of the twin spicule and part of the ascending loop. (Fig. 2, 15:10:09–15:12:33). A loop-like feature is also visible at the He I D_3 line (Fig. 3: 15:10:21). The plasma blob is moving along the limb towards the right as we observe (northward). Near the end of the main phase we observe material ejected along the arch at the base of the configuration (Fig. 2: 15:12:33, 15:12:57 and Fig. 4: 15:11:53, 15:12:17) and also along other arch-shaped trajectories.

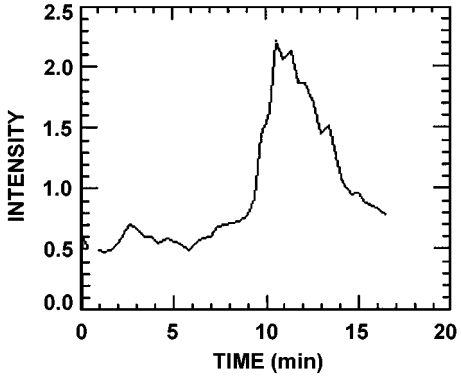

Fig. 5. Light curve (computed from the Hα center images) of the region of the intense brightening related to the polar surge. Note the asymmetry of the profile confirming the impulsive nature of the event

3.2. Intensity enhancement

Figure 5 shows the intensity curve of the region where the intense brightening associated with the polar surge first appeared (6.5 Mm above the photospheric limb). The maximum value of the intensity was about four times the background intensity (without any correction for smearing). The lifetime of the brightening at that region was about 6 min. The strong intensity enhancement indicates a heating in high temperatures of the lifted material. In combination with the high velocity found (cf. next section), this suggests that an explosive event is taking place.

3.3. Dynamics of the polar surge

In order to study the dynamics of the polar surge we computed velocities based on two methods; i) the apparent displacement of structures (proper motions), and ii) by using a "three wavelengths" method to evaluate Doppler motions.

From the apparent displacement of the emerging loop we found that its propagation velocity is about 52 $\mathrm{km\,s^{-1}}$. The bright blob of material is propagating with a mean velocity of about 48 $\mathrm{km\,s^{-1}}$. The propagation shows a large acceleration (approximately 0.5 $\mathrm{km\,s^{-2}}$). The mean ejection velocity along the arch-shaped loop at the base of the configuration (observed after the main phase) is about 46 $\mathrm{km\,s^{-1}}$; the flow shows an acceleration just after the apex of the arch followed by a deceleration.

A popular method to determine of the physical properties of chromospheric features using Hα filtergrams is Beckers' cloud model (Beckers 1964). This model takes into account four parameters: the source function, the optical depth at line center, the Doppler width which depends on the temperature and the microturbulent motions, and the Doppler shift corresponding to the line-of-sight component of the mass velocity. All parameters are assumed to be constant along the line of sight through the structure. Furthermore, the source function is assumed to be wavelength-independent and the profile of the optical depth is assumed Gaussian. We adopt the same nomenclature, but assume that the profile of the overlimb structures is a pure Doppler-broadened emission profile with a nearly Gaussian shape. In that case the intensity profile $I(\Delta\lambda)$ of Hα can be written as follows:

$$I(\Delta\lambda) = I_{\mathrm{c}} \exp(-(\lambda/\Delta\lambda_{\mathrm{D}})^2(\Delta\lambda/\lambda - u/c)^2) \quad (1)$$

where I_{c} is related to the source function and the optical depth at line center, λ is the wavelength, $\Delta\lambda_{\mathrm{D}}$ is the Doppler width and u is the flow velocity (positive towards the observer). Assuming that the intensity profile is symmetric with respect to the line center and if we denote $I_+ = I(\Delta\lambda)$, $I_- = I(-\Delta\lambda)$ and I_0 the intensity at line center, we can eliminate I_{c} and obtain the relation:

$$u = \frac{c\Delta\lambda}{2\lambda} \frac{\ln(I_+/I_-)}{\ln(I_+ I_-/I_0^2)}. \quad (2)$$

As can readily be seen, the variables at the right-hand side of the above equation can be determined from observations in three wavelengths. A similar model was used by Malherbe et al. (1997) for the computation of velocities related to the evolution of Hα postflare loops.

Figure 6 shows the evolution of the velocity field. There are points (easily discernible) where the method fails to successfully compute the velocities, due to the fact that the Gaussian profile assumption is no longer valid (as in the case of overlapping structures. The line of sight velocities computed from the "three wavelengths" method are appreciably smaller than those estimated from the apparent displacement of the structures. This is mainly due to projection effects; however an underestimation of the velocity due to the "three wavelengths" method is also possible.

The line of sight velocity of the ascending loop is about -5 $\mathrm{km\,s^{-1}}$ during the initial phases of the rising and reaches -7.5 $\mathrm{km\,s^{-1}}$ during the final stages. This difference should be related to projection effects and does not reflect a real acceleration. The loop is not vertical but inclined to the left side of the configuration. During the explosive phase of the event, velocities of the order of 25 $\mathrm{km\,s^{-1}}$ were observed around the explosive points. We should, however, note that at the explosion points our model collapsed. From the asymmetry observed in the two wings, the line of sight velocities should be higher than 30 $\mathrm{km\,s^{-1}}$. The values of the velocity of the bright blob are very small, of the order of 1–3 $\mathrm{km\,s^{-1}}$. Initially the velocity is positive and then became negative. This indicates that the propagation direction of the blob should be almost orthogonal to the line of sight; a turbulent motion is possible. The line of sight velocity in the arch-shaped loop observed after the main phase of the phenomenon is near -4.5 $\mathrm{km\,s^{-1}}$ during the initial phase of the ejection, just before the apex of the structure. After the apex it is -6 $\mathrm{km\,s^{-1}}$ and in a later stage it reaches -11.5 $\mathrm{km\,s^{-1}}$. Finally, at the lower parts of the loop it is reduced to about -3 $\mathrm{km\,s^{-1}}$. This behavior is more consistent with a siphon flow than a ballistic ejection.

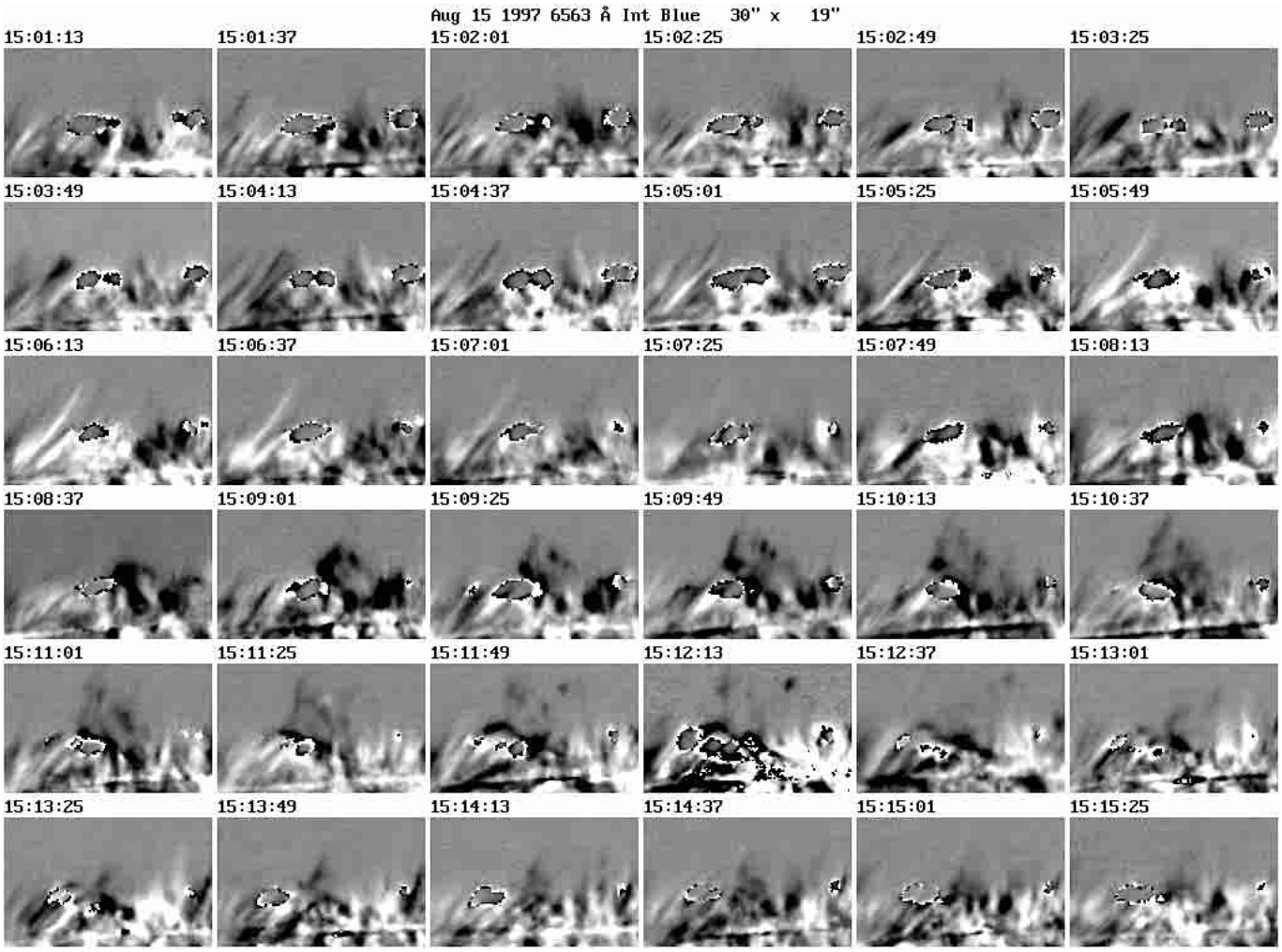

Fig. 6. Velocity images computed using the "three wavelengths" method showing the evolution of the velocity field of the same region as in Fig. 2. Velocity values are scaled so that extreme dark corresponds to -3 km s^{-1} or greater values and extreme bright to 3 km s^{-1} or greater values. Points where the model fails to compute the velocity successfully are obvious; they are mainly located near the top of the loop. At these points, the Gaussian profile assumption is no longer valid and optical depth effects are produced

Figure 7 shows enlarged velocity images around the main phase of the phenomenon. We noted a cloud of material leaving the polar surge with similar velocities, clearly above the background noise and different from the spicules behind it. The cloud is produced after the main phase and is similar to the signature we usually see in He II images.

3.4. Comparison to theoretical models

Yokoyama & Shibata (1993, 1995) performed numerical simulations of solar coronal X-ray jets based on a model of magnetic reconnection between emerging flux and the preexisting coronal magnetic field (YS model). According to their 2-D model, a magnetic loop emerges in the atmosphere due to magnetic buoyancy instability with a rising velocity of the order of 6–10 km s^{-1}. When the top of the rising loop enters the coronal level a current sheet is created between the loop top and the coronal field. Magnetic islands that confine cool, dense, chromospheric plasma are created in the current sheet by a tearing instability; they are finally ejected with a velocity of about 36 km s^{-1}. A pair of reconnection jets are ejected from the neutral point; one of these pair of jets ascends and collides with the magnetic field lines finally creating a hot jet. In addition to the upward ejection of the hot jet cool plasma, the plasma that is carried up with the expanding loops, is ejected by a sling-shot effect due to reconnection, which produces a whip-like motion with a velocity between 48–84 km s^{-1}. The final configuration of the cool plasma is a vertical collimated feature, which may be observed as a cool jet.

We propose that a similar scenario applies in the case of the polar surge that we have observed, although we lack observations of the hot plasma phenomena and suggest that a 3-D geometry is more appropriate to describe it. The event started with the rising of a bright loop carrying up chromospheric material. The ascending velocity of the loop reached 50 km s^{-1}, which is higher than that predicted by the YS model. An intense brightening was

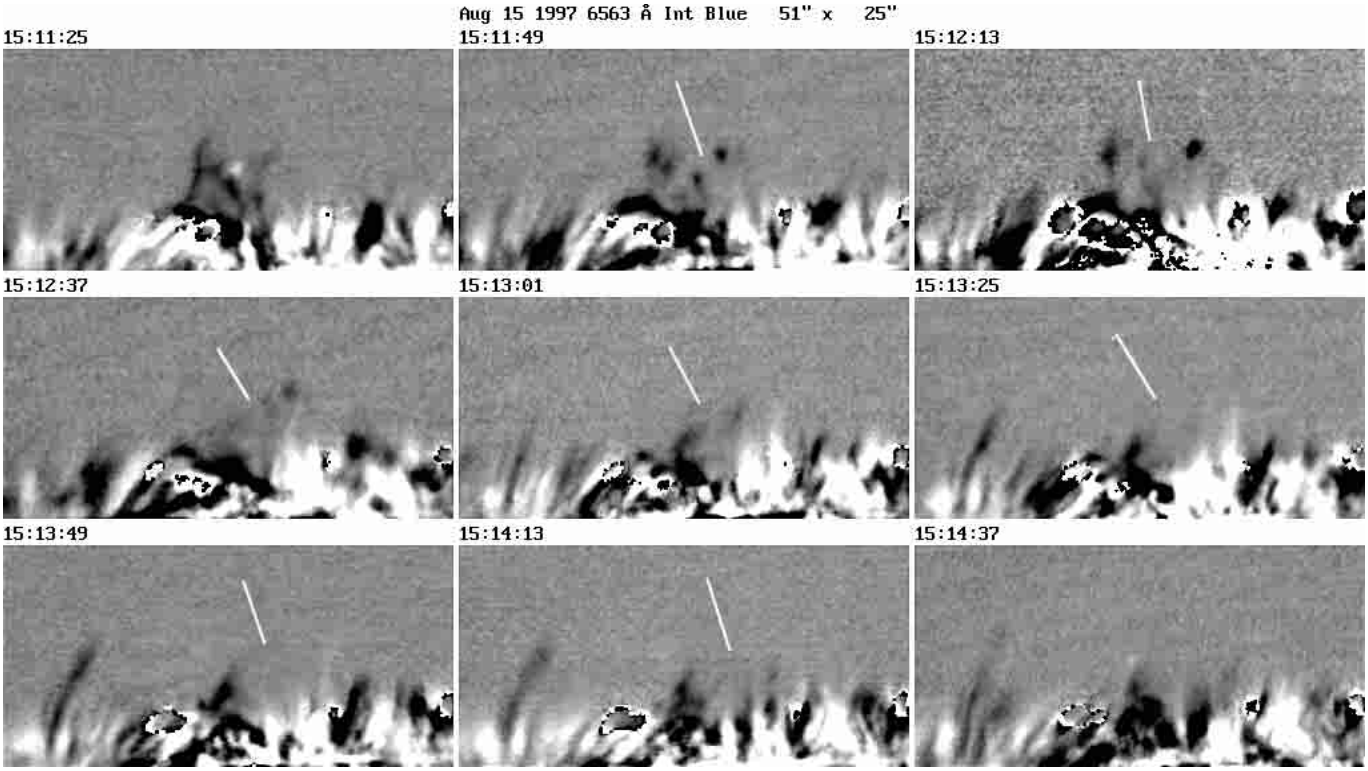

Fig. 7. Enlarged velocity images (computed using the "three wavelengths" method) after the main phase of the phenomenon. Extreme dark corresponds to -1.5 km s^{-1} or greater values and extreme bright to 1.5 km s^{-1} or greater values. We have marked a cloud of material rapidly leaving from the region with velocities clearly above the background noise and different from that of the spicules behind it

observed near the contact point of the rising loop and the remnants from the twin spicule, probably where a neutral point was created. Subsequently, a bright blob was created which moved away with a velocity of about 48 km s^{-1}. It could be attributed to the formation of a magnetic island; the propagation velocity is similar to that predicted by the YS model. A cloud of material was ejected towards the same direction as the bright blob, probably due to a slingshot ejection related to a whip-like motion of the magnetic field lines. Finally, ejection of cool material carried up by the ascending loop was observed. The material was ejected both vertically and along arch-shaped loops at the base of the configuration.

This scenario is also consistent with our findings in Paper I, that polar surges observed in Hα have corresponding structures in He II, but that the geometry and the length of the corresponding spikes are not the same.

Finally, we would like to point out that a scenario which has been proposed by Antiochos et al. (1999) for CME-type events could also fit with what we have observed, assuming that a rescaling to smaller sizes is possible. In that case, the reconnection in the corona is produced as a result of the shearing in two magnetic regions forming a quadrupole configuration. The darkening we observe here could be similar to the cavity which is known to evolve and erupt during a CME event.

3.5. Comparison to polar surges observed with medium resolution

It is clear that not all macrospicules should be related to this class of events (only a subcategory are related to explosive phenomena). According to the description of Moore et al. (1977), the most common structural form of the events they observed was an erupting arch, the top of which usually becomes extended or opens. Often an event is initiated by a sudden flarelike brightening in the chromosphere at the limb and during the rise phase the eruption is usually brighter than the normal Hα chromosphere at the limb. According to Koutchmy & Loucif (1991) a group of the events they studied evolve as rising domes and after reaching a certain height they eject part of their mass. Karovska & Habbal (1994), from the analysis of EUV observations obtained in the C III 977 Å line, found that macrospicules often consist of column-like structures with low-lying arches at their bases. According to their description, archlike structures are often formed due to interactions between fine structures. Occasionally, the archlike structure formation is followed by expulsion of material and formation of macrospicules. Finally, in Paper I (Fig. 3), we presented the appearance, development and decay of a characteristic polar surge observed on December 13 under medium resolution.

From the comparison of the above-mentioned descriptions (and the corresponding images) with our high

resolution example, there are several common evolutionary characteristics that can help in forming an integrated picture of polar surges:
1) The events start with the eruption of a bright loop (archlike or domelike feature) carrying up chromospheric material;
2) Upon reaching a certain height, an intense flarelike brightening is observed, related to an explosive event;
3) After the explosive event, upward ejection of material and formation of bright blobs (small roundish clouds of material) are observed;
4) The reorganization of loops and ejection of material along arch shaped loops at the base of the polar surges is observed most likely as a transverse expansion of the mountlike configurations;
5) SXR emission of a typical X-ray bright point is observed at the location of the polar surges which eventually could be recurrent.

4. Summary and conclusions

We presented a representative example of a polar surge observed under exceptionally high resolution. Although this is the only example we were able to observe at such high resolution, all polar surges present morphological characteristics similar to this example.

Before the numerical simulations of Yokoyama and Shibata, it had long been thought that cool Hα plasma ejection could not be explained by magnetic reconnection because reconnection would heat any cool plasma to X-ray temperatures. However, according to their model there are four types of jet-like flow associated with the reconnection: hot jet along the magnetic field lines, slingshot jet, simple island ejection, and surge-like cool jet. Wilhelm (2000) concluded that his findings from SUMER observations were not consistent with any mechanism which requires a field-aligned direction of the macrospicule propagation. Thus, he proposed that their generation is related to an explosive event occurring during the magnetic reconnection phase of a network loop system, with another such system or with a unipolar-field region of appropriate polarity. He suggested that the chromospheric material is carried up by the relaxing magnetic field following the field-line reconnection (see his Fig. 8).

The dynamics of the polar surge we analyzed is consistent with reconnection theory models presented for SXR-jet phenomena (Yokoyama & Shibata 1993, 1995, see also Fig. 14 of Shibata 1998). As shown here, even above a polar region, where the surrounding field is nearly radial, small-scale erupting and explosive sites exist well above the chromosphere. Our analysis strongly supports the hypothesis that magnetic reconnection, triggered by emerging flux, provides the accelerative mechanism for this kind of macrospicules. An alternative possibility is the shearing, by intermediate scale photospheric motions of the footpoints of the underlying complex structure of the magnetic field, to trigger the eruption (Antiochos et al. 1999). A three dimensional theoretical model and coordinated ground-based and space observations are necessary for a more detailed comparison. An even more powerful analysis from different points of view will be possible from observations collected with the Solar Probe planned to fly over the poles at 10 to 4 Solar radii distances.

Acknowledgements. We would like to thank Dr. R. N. Smartt, the T.A.C. of NSO/SP and the staff of the Sacramento Peak Observatory for their warm hospitality and their help obtaining the observations. Further, we would like to thank the referee (Dr. H. Wöhl) for his suggestions that helped improve the paper. This work was partially supported by NSF grant ATM-9726147.

References

Antiochos, S. K., DeVore, C. R., & Klimchuk, J. A. 1999, ApJ, 510, 485
Beckers, J. M. 1964, Ph.D. Thesis, Utrecht
Bohlin, J. D., Vogel, S. N., Purcell, J. D., et al. 1975, ApJL, 197, L133
Blake, M. L., & Sturrock, P. A. 1985, ApJ, 290, 359
Chae, J., Qiu, J., Wang, H., & Goode, P. R. 1999, ApJ, 513, L75
Christopoulou, E. B., Georgakilas, A. A., & Koutchmy, S. 2001, Solar Phys., in press
Gaizauskas, V. 1996, Solar Phys., 169, 357
Georgakilas, A. A., Koutchmy, S., & Alissandrakis, C. E. 1999, A&A, 341, 610, Paper I
Godoli, G., & Mazzuconi, F. 1967, ApJ, 147, 1131
Karovska, M., & Habbal, R. S. 1994, ApJ, 431, L59
Kurokawa, H., & Kawai, G. 1993, in The Magnetic and Velocity Fields of Solar Active Regions, ed. H. Zirin, G. Ai, & H. Wang, ASP Conf. Ser., 46, 507
Koutchmy, O., & Koutchmy, S. 1989, in High Spatial Resolution Solar Observations, ed. O. von der Lühe, Proceedings of the 10th Sacramento Peak summer Workshop 46, 217
Koutchmy, S., & Loucif, M. L. 1991, in Mechanisms of Chromospheric and Coronal Heating, ed. P. Ulmschneider, E. R. Priest, & R. Rosner, Proceedings of the Heidelberg Conference, 152
Loucif, M. L., Koutchmy, S., Stellmacher, G., et al. 1998, in Solar Jets and Coronal Plumes, Guadeloupe International meeting, ed. T.-D., Guyenne, ESA SP-421, 299
Moe, O. K., Engvold, O., & Beckers, J. M. 1975, Solar Phys., 40, 65
Malherbe, J.-M., Tarbell, T., Wiik, J. E., Schmieder, B., & Frank, Z. 1997, ApJ, 482, 535
Moore, R. L., Tang, F., Bohlin, J. D., & Golub, L. 1977, ApJ, 218, 286
Shibata, K. 1998, in Solar Jets and Coronal Plumes, Guadeloupe International meeting, ed. Guyenne T.-D., ESA SP-421, 137
Wang, H. 1998, ApJ, 509, 461
Wilhelm, K. 2000, A&A, 360, 351
Yokoyama, T., & Shibata, K. 1993, in ESA, Fourth International Tokio Conference on Plasma Physics and Controlled Nuclear Fusion, 203
Yokoyama, T., & Shibata, K. 1996, PASJ, 48, 353
Zirin, H., & Cameron, R. 1998, in Solar Jets and Coronal Plumes, Guadeloupe International meeting, ed. Guyenne T.-D., ESA SP-421, 39